Altered stress stimulation of inward rectifier potassium channels in Andersen-Tawil syndrome

Guiscard Seebohm,[*,1,2] Nathalie Strutz-Seebohm,[*,1] Oana N. Ursu,[‡] Regina Preisig-Müller,[§] Marylou Zuzarte,[§] Elaine V. Hill,[¶] Marie-Cécile Kienitz,[†] Said Bendahhou,[#] Michael Fauler,[**] Daniel Tapken,[††] Niels Decher,[‖] Anthony Collins,[‡‡] Karin Jurkat-Rott,[**] Klaus Steinmeyer,[§§] Frank Lehmann-Horn,[**] Jürgen Daut,[§] Jeremy M. Tavaré,[¶] Lutz Pott,[†] Wilhelm Bloch,[‖‖] and Florian Lang[‡]

[*]Department of Biochemistry I and [†]Department of Cellular Physiology, Ruhr University Bochum, Bochum, Germany; [‡]Institute of Physiology I, University of Tübingen, Tübingen, Germany; [§]Institute of Physiology and [‖]Vegetative Physiology, University of Marburg, Marburg, Germany; [¶]Department of Biochemistry, School of Medical Sciences, University of Bristol, Bristol, UK; [#]Unité Mixte de Recherche (UMR) 6097 Centre National de la Recherche Scientifique (CNRS) Transport Ionique Aspects Normaux et Pathologiques (TIANP), Université de Nice Sophia Antipolis, Nice, France; [**]Division of Neurophysiology, Ulm University, Ulm, Germany; [††]Department of Medicinal Chemistry, Faculty of Pharmaceutical Sciences, University of Copenhagen, Copenhagen, Denmark; [‡‡]Centre for Vision and Vascular Science, Institute of Clinical Science, Queen's University Belfast, Belfast, UK; [§§]Sanofi-Aventis, Therapeutic Strategic Unit (TSU) Aging, Frankfurt am Main, Germany; and [‖‖]German Sport University Cologne, Cologne, Germany

ABSTRACT **Inward rectifier potassium channels of the Kir2 subfamily are important determinants of the electrical activity of brain and muscle cells. Genetic mutations in Kir2.1 associate with Andersen-Tawil syndrome (ATS), a familial disorder leading to stress-triggered periodic paralysis and ventricular arrhythmia. To identify the molecular mechanisms of this stress trigger, we analyze Kir channel function and localization electrophysiologically and by time-resolved confocal microscopy. Furthermore, we employ a mathematical model of muscular membrane potential. We identify a novel corticoid signaling pathway that, when activated by glucocorticoids, leads to enrichment of Kir2 channels in the plasma membranes of mammalian cell lines and isolated cardiac and skeletal muscle cells. We further demonstrate that activation of this pathway can either partly restore (40% of cases) or further impair (20% of cases) the function of mutant ATS channels, depending on the particular Kir2.1 mutation. This means that glucocorticoid treatment might either alleviate or deteriorate symptoms of ATS depending on the patient's individual Kir2.1 genotype. Thus, our findings provide a possible explanation for the contradictory effects of glucocorticoid treatment on symptoms in patients with ATS and may open new pathways for the design of personalized medicines in ATS therapy.—Seebohm, G., Strutz-Seebohm, N., Ursu, O. N., Preisig-Müller, R., Zuzarte, M., Hill, E. V., Kienitz, M.-C., Bendahhou, S., Fauler, M., Tapken, D., Decher, N., Collins, A., Jurkat-Rott, K., Steinmeyer, K., Lehmann-Horn, F., Daut, J., Tavaré, J. M., Pott, L., Bloch,W., Lang, F. Altered stress stimulation of inward rectifier potassium channels in Andersen-Tawil syndrome. *FASEB J.* 26, 513–522 (2012). www.fasebj.org**

Key Words: oocytes · PIP_2 · trafficking · PIP5K3 · Kir2

Potassium channels of the Kir2 (*KCNJ,* IRK) subfamily are critical for stabilization of the resting membrane potential of excitable cells such as cardiac and skeletal myocytes and neurons (1). The three subunits Kir2.1, Kir2.2, and Kir2.3 are highly expressed in the heart, where they also appear to form heteromeric channels that conduct the inwardly rectifying I_{K1} current, a major determinant of the resting membrane potential and of the late action potential repolarisation phase (1–3). The importance of Kir2 channels for cardiac function is highlighted by a gain-of-function mutation causing atrial fibrillation (3) and by reduced I_{K1} in heart failure (4–7). Kir2 channels may also provide the functional link between mitochondrial dysfunction and altered membrane excitability (8, 9).

Andersen-Tawil syndrome (ATS; refs. 10–12) is a rare familial disorder characterized by potassium-sensitive periodic paralysis, ventricular arrhythmia, and dysmorphic features such as syndactyly and altered face shapes. Cardiac electropathophysiology includes variable QT interval prolongation and abnormal T-wave morphology, often presenting with very prominent U waves (13, 14). In a large ATS family, the disease was mapped to the chromosomal locus 17q, and in a

[1] These authors contributed equally to this work.

[2] Correspondence: Department of Biochemistry I–Cation Channel Group, Ruhr University Bochum, Universitätsstraße 150, 44780 Bochum, Germany. E-mail: guiscard.seebohm@gmx.de

doi: 10.1096/fj.11-189126

This article includes supplemental data. Please visit *http://www.fasebj.org* to obtain this information.

candidate gene approach, missense mutations were identified in the *KCNJ2* gene encoding for Kir2.1 (13).

Kir2 channels are modulated and regulated in multiple ways. Kir2.1, for instance, is directly regulated by arachidonic acid, cholesterol, and phosphatidylinositol-4,5-bisphosphate [$PI(4,5)P_2$] (2, 15–18). Several ATS-associated mutations in Kir2.1 disrupt PIP_2 binding and thus render channels insensitive to PIP_2-dependent stimulation (19). Kir2 channels are also regulated by kinases, *e.g.*, PKC, which down-regulates all three subunits (20); PKA, which up-regulates Kir2.2; and tyrosine kinases, which down-regulate Kir2.1 (21, 22). Moreover, a variety of proteins regulate Kir2 channel trafficking, *e.g.*, Rho, AKAP79, SAP97, TNF-α, Chapsyn 110, filamin-A, PSD95, CASK, Veli, and Mint1 (21, 23–30). Several of these kinases and interacting proteins may link hormonal signaling systems to Kir2 function, but detailed molecular information on hormone-modulated recycling of Kir2 channels is still missing.

MATERIALS AND METHODS

Molecular biology

The cDNAs of guinea-pig Kir2.1, Kir2.2, and Kir2.3 cloned into the oocyte expression vector pSGEM and the construction of ATS mutants of Kir2.1 have been described previously (2, 3). To facilitate domain exchange in the creation of chimeras between Kir2.1 and Kir2.2, we introduced *Bam*HI sites. In the cases when introduced *Bam*HI sites resulted in Kir2.1/Kir2.2 divergent sequences within the *Bam*HI sites, these divergent sequences were later mutated back according to the original Kir2.1/Kir2.2 sequence. Site-directed mutagenesis was performed with the QuikChange Site-Directed Mutagenesis Kit (Stratagene, La Jolla, CA, USA). Template Kir2, phosphoinositide-3-phosphate-5-kinase 3 (PIP5K3), and serum- and glucocorticoid-inducible kinase 1–3 (SGK1–3) cDNAs were linearized with an appropriate restriction enzyme, and cRNA was synthesized from 1 μg of linearized DNA using the mMessage mMachine T7 or SP6 *in vitro* transcription kits (Ambion, Austin, TX, USA; ref. 31). The cRNA concentrations were photometrically determined, and transcript quality was checked by agarose gel electrophoresis.

Electrophysiological studies in *Xenopus* oocytes

To obtain oocytes, ovarian lobes were harvested from *Xenopus laevis* anesthetized with a 0.17% tricaine solution, as described previously (32, 33). Follicle cells were removed by treatment with collagenase (1 mg/ml, type II; Worthington, Lakewood, NJ, USA) in Ca^{2+}-free ND96 solution (96 mM NaCl, 2 mM KCl, 2 mM $MgCl_2$, and 5 mM HEPES, pH 7.6) for 2 h. Oocytes were then maintained at 17°C in ND96 containing 50 μg/ml gentamicin, 0.5 mM theophylline, and 2.5 mM sodium pyruvate. Oocytes were injected with 1 ng Kir2 cRNA plus, if applicable, 3 ng SGK3 or 2 ng PIP5K3 cRNA.

At 2 d after injection, currents were recorded at room temperature with a Turbo Tec-10CX amplifier (NPI Electronic, Tamm, Germany) using standard 2-electrode voltage clamp techniques (33). Pipettes were filled with 3 M KCl and had resistances of 0.3–0.8 MΩ. For all experiments, the integrator was set to 2–3 ms to enable good clamp performance, and the clamp was controlled *via* the PI controller. Data were Bessel-filtered at 500 Hz and digitized with a sampling rate of 2 kHz. The recording solution KD60 contained 60 mM KCl, 38 mM NaCl, 1.8 mM $CaCl_2$, 2 mM $MgCl_2$, and 5 mM HEPES and was equilibrated to pH 7.5. Specific pulse protocols are described in the figures.

Chemiluminescence detection of surface proteins in oocytes

Experiments were performed as described previously (31–33). Oocytes expressing Kir2.1 containing a hemagglutinin (HA) epitope in the extracellular loop after position 117 of the mature protein were incubated for 30 min in ND96 with 1% BSA at 4°C to block nonspecific antibody binding. Oocytes were subsequently incubated for 1 h at 4°C with a rat monoclonal anti-HA antibody (Roche, Mannheim, Germany; 1 μg/ml plus 1% BSA in ND96), washed 5 times at 4°C with 1% BSA in ND96, and then incubated with 2 μg/ml peroxidase-conjugated affinity-purified $F(ab')_2$ fragment goat anti-rat IgG antibody (Jackson ImmunoResearch, Newmarket, Suffolk, UK) in 1% BSA/ND96 for 1 h. Oocytes were thoroughly washed 10 times for 5 min at 4°C in 1% BSA/ND96 and then 5 times in ND96 without BSA for 5 min at 4°C. Individual oocytes were transferred to 20 μl SuperSignal ELISA Femto Maximum Sensitivity Substrate (Pierce, Rockford, IL, USA), and chemiluminescence of single oocytes was measured with a Wallac Victor 2 plate reader (Perkin Elmer, Waltham, MA, USA). The results from 3 independent experiments were averaged (60 oocytes), and data are presented in relative light units.

In vitro phosphorylation assay

In vitro phosphorylation was performed as described previously, with N-terminally truncated wild-type or mutant PIP5K3 (aa 1-497) expressed as a recombinant fusion protein with glutathione *S*-transferase (GST) in *Escherichia coli* (32). Briefly, 1 L of *E. coli* was grown to an optical density (A_{600}) of 0.8, and protein expression was induced over 2 h by the addition of 0.5 mM isopropyl-β-D-thiogalactopyranoside. The cells were harvested by centrifugation, resuspended in 40 ml of ice-cold lysis buffer (50 mM Tris, pH 7.5; 1% Triton X-100; 150 mM NaCl; 5 mM $MgCl_2$; 1 mM dithiothreitol; and 0.2 mM phenylmethylsulfonyl fluoride), and lysed by sonication. Insoluble material was removed by centrifugation, and GST-PIP5K3 protein was affinity purified with glutathione-sepharose beads. The purified GST-PIP5K3 protein was incubated with 20 mU PKB or SGK3 (Upstate Technology, Lake Placid, NY, USA) in phosphorylation buffer [20 mM MOPS, pH 7.2; 1 mM EDTA; 0.1% β-mercaptoethanol; 20 mM β-glycerophosphate; 10 mM $MgCl_2$; and 500 mM ATP (0.05 MBq [γ-^{32}P]ATP/sample)] at 30°C for 20 min. Sample buffer was added, and the samples were heated at 95°C for 5 min. Proteins were separated by SDS-PAGE on a 4–12% Bis-Tris gel and transferred to a PVDF membrane. Incorporation of radioactively labeled phosphate was analyzed by autoradiography, and proteins were detected with an anti-GST antibody.

Expression and detection of EGFP-tagged Kir2.2 in HeLa or HEK293 cells

HeLa cells maintained at 37°C and 5% CO_2 in cell culture medium containing 10% FCS were plated on glass-bottom dishes (Willco Wells, Amsterdam, The Netherlands); 1 d later, they were transfected with 0.5 μg of EGFP-tagged Kir2.2 cDNA using Lipofectamine (Invitrogen, Carlsbad, CA, USA) according to the manufacturer's instructions. After 4–6 h, the medium was replaced by serum-free medium, and the cells were incubated for another 4–6 h. Endogenous SGK1

was then stimulated by exchanging the medium for medium containing 10% FCS and 3 μM dexamethasone, while control cells were treated with fresh serum-free medium. EGFP fluorescence was recorded after addition of serum and dexamethasone with an IX71 microscope (Olympus, Hamburg, Germany) equipped with a 12-bit CCD camera (SensiCam QE; PCO, Kelheim, Germany) for the time-lapse video (Supplemental Video S1) using a ×100 objective, an HQ 525/50 emission filter, and a 6% neutral density filter to reduce bleaching. The objective was heated to 37°C with an objective heater (Bioptechs, Butler, PA, USA).

HEK293 cells cultured at 37°C and 5% CO_2 in cell medium containing 10% FCS were plated on glass coverslips and transfected with 1 μg of EGFP-tagged Kir2.2 cDNA using FuGene 6 (Roche, Mannheim, Germany) according to the manufacturer's instructions. After 24 h, endogenous SGK was stimulated with medium containing 10% FCS and 3 μM dexamethasone, while control cells were maintained in serum-free medium. EGFP fluorescence was detected with an Optiphot microscope (Nikon, Kingston, UK) equipped with a spot camera system (Visitron, Puchheim, Germany) using a ×40 objective and an appropriate filter set. The images were processed using Image-Pro Plus 4.5 (MediaCybernetics, Bethesda, MD, USA) and analyzed using ImageJ (U.S. National Institutes of Health, Bethesda, MD, USA).

Isolation and cultivation of adult rat atrial myocytes

Wistar Kyoto rats of either sex were killed following protocols approved by the animal welfare officer of the Ruhr University Bochum in accordance with the guidelines of the European Community (86/609/EEC). Wistar-Kyoto rats of either sex (weight ~200 g) were anesthetized by intravenous injection of urethane (1 g/kg). The chest was opened, and the heart was removed and mounted on the cannula of a Langendorff perfusion system for coronary perfusion at constant flow. Atrial myocytes were isolated enzymatically, as described previously (35) and then plated at a low density (several hundred cells per dish) and routinely cultured in FCS-free medium (HEPES-buffered M199; PAA Laboratories, Pösching, Austria) supplemented with insulin/transferrin/selenium, gentamicin (1.4 μg/ml; Sigma-Aldrich, München, Germany), and kanamycin (0.7 μg/ml; Sigma-Aldrich). The medium was changed every second day.

Current recordings in cardiac myocytes

For whole-cell patch-clamp measurements of membrane currents, an extracellular solution of the following composition was used: 120 mM NaCl, 20 mM KCl, 0.5 mM $CaCl_2$, 1.0 mM $MgCl_2$, and 10.0 mM HEPES/NaOH (pH 7.4). The pipette solution contained 110 mM K-aspartate, 20 mM KCl, 5.0 mM NaCl, 1.0 mM $MgCl_2$, 5.0 mM Na_2ATP, 2.0 mM EGTA, 25 μM GTP, and 10.0 mM HEPES/KOH (pH 7.4). The K^+ reversal potential under these condition was calculated as −48 mV. Standard chemicals were from Merck (Darmstadt, Germany). EGTA, HEPES, Na_2ATP, and GTP were from Sigma-Aldrich. Membrane currents were measured at ambient temperature (22–24°C) using standard whole-cell patch clamp software ISO2 (MFK, Niedernhausen, Germany). Cells were voltage clamped at a holding potential of −90 mV, *i.e.*, negative to E_K, resulting in inward K^+ currents. Every 10 s, voltage ramps (duration 500 ms) from −120 to +60 mV were applied to assess stability of the recording conditions (membrane currents in response to depolarizing voltage ramps are shown as downward deflections). Rapid exposure to extracellular solutions was performed by means of a custom-made solenoid-operated flow system permitting a change of solution around an individual cell with a half time of ~100 ms. At 24 h after cell isolation, myocytes were incubated with M199 medium containing 10% FCS and 100 nM dexamethasone for 2 h. Measurements were performed >48 h after cell incubation with FCS/dexamethasone. Time-matched sister cultures served as controls. For measurements cells devoid of contact with neighboring cells were selected.

Data analysis

Data were analyzed utilizing Clampfit 8 (Axon Instruments, Foster City, CA, USA) and Origin 6 (OriginLab, Northampton, MA, USA) software. Student's *t* test or ANOVA was used to test for statistical significance. A value of $P < 0.05$ was considered statistically significant. Numerical values are reported as means ± SE (n=number of experiments).

Computer modeling

A 2-compartment computer model of resting membrane potential generation was developed. Details are given in Supplemental Data.

RESULTS

Activation of endogenous SGK1 stimulates native I_{K1} in atrial myocytes

Atrial myocytes contain a native I_{K1} that can be distinguished from the total background current by its sensitivity to low concentrations of Ba^{2+} (36). The amplitude of the 2 μM Ba^{2+}-sensitive I_{K1} current of isolated atrial myocytes was relatively small when cells were cultured in serum/dexamethasone-free medium, whereas its density increased >2-fold when cells were cultured in the presence of serum and dexamethasone, suggesting that activation of a serum- and glucocorticoid-inducible gene like the candidate gene SGK stimulates endogenous Kir channels in atrial myocytes (**Fig. 1**).

Kir2.2-mediated currents are increased by SGK1–3

To test the hypothesis that SGK1–3 stimulate Kir2 channels, we compared current amplitudes of Kir2.1, Kir2.2, and Kir2.3 expressed in *Xenopus* oocytes alone or together with individual SGK isoforms. The 2-electrode voltage-clamp technique in high extracellular potassium concentration was used. Kir2.2-mediated currents were significantly increased (2.5- to 4-fold) by coexpression of SGK1, SGK2, or SGK3, whereas Kir2.1 and Kir2.3 were not significantly stimulated by coexpression of SGKs (**Fig. 2*A*, *B***).

To determine whether the potentiation of Kir2.2-mediated currents by SGKs requires kinase activity, we coexpressed the Kir2.2 channels with either constitutively active (SD) or inactive (KN) mutants of SGK1 or SGK3. The constitutively active kinases but not the inactive kinases were able to stimulate Kir2.2 channels (Fig. 2*C*), strongly suggesting that SGK1 and SGK3 exert their effects on Kir2.2 by phosphorylation.

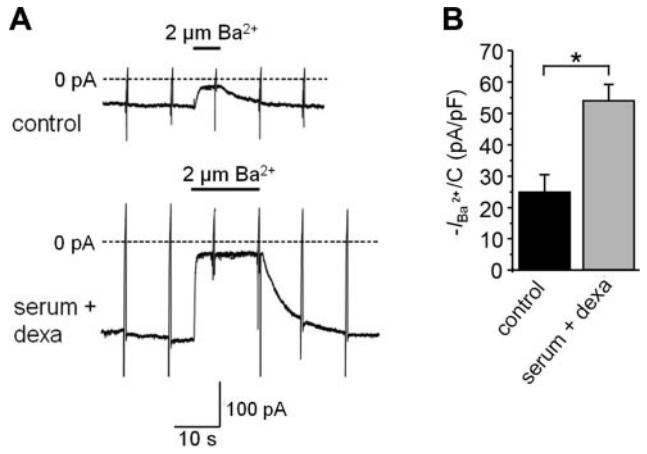

Figure 1. Activation of SGK1 increases native inwardly rectifying background currents in cardiac myocytes. *A*) Representative traces of background potassium currents in rat atrial myocytes incubated in the absence of serum and dexamethasone (top trace) or incubated with culture medium supplemented with 10% FCS (serum) and 100 nM dexamethasone (dexa) for 2 h to stimulate SGK1 expression (bottom trace). Rapid deflections represent responses to voltage ramps from −120 to +60 mV, which were applied every 10 s to assess stability of the recording conditions. Cells were superfused for the indicated time with 2 μM Ba^{2+} to selectively block the Kir2-generated current. *B*) Summarized current densities of the barium-sensitive ($I_{Ba}{}^{2+}$/C) current (n=8–10). Stimulating effect of serum + dexamethasone was recorded ~48 h after incubation. *$P < 0.05$.

PIP5K3 phosphorylation is crucial for stimulation of Kir2.2 by SGK3

It has recently been reported that PKB and SGK1 phosphorylate PIP5K3 at position 318, thus stimulating its kinase activity (22). Similar to PKB and SGK1, SGK3 preferentially phosphorylates motifs containing arginines at positions 3 and 5 relative to the S/T phosphorylation site (consensus motif, RxRxxS/T; ref. 22). By *in vitro* phosphorylation with [γ-^{32}P]ATP and subsequent Western blot analysis, we demonstrated that PIP5K3 is indeed also phosphorylated by SGK3 (**Fig. 3*A***). By contrast, only very weak phosphorylation of the PIP5K3(S318A) mutant was observed, indicating that, as predicted, phosphorylation by SGK3 takes place at residue S318.

To test whether the stimulation of Kir2.2 by SGK3 depends on phosphorylation of PIP5K3, we coexpressed Kir2.2 with SGK3 and either wild-type PIP5K3 or PIP5K3(S318A). SGK3 increased Kir2.2-mediated current amplitudes to the same extent regardless of the exogenous presence or absence of wild-type PIP5K3 (Fig. 3*B*), whereas overexpression of mutant PIP5K3(S318A) (and thereby outcompeting endogenous PIP5K3) disrupted the stimulatory effect of SGK3 on Kir2.2 completely. These results suggest that SGK3 stimulates Kir2.2 channels *via* activation of PIP5K3 by S318 phosphorylation.

Activated PIP5K3 was recently reported to generate PI(3,5)P_2 *in vitro* (22). Along those lines, we found that injection of PI(3,5)P_2 into *Xenopus* oocytes activated Kir2.2 but not Kir2.1 or Kir2.3 (Fig. 3*C*).

C terminus and a part of the N terminus of Kir2.2 determine SGK3 sensitivity

To identify the domains in Kir2.2 conferring SGK3 sensitivity, we constructed a set of Kir2.1/Kir2.2 chimeras (**Fig. 4**). We found that the stimulatory effect of SGK3 on Kir2.2 current amplitudes was abolished when either the C terminus or the first 78 residues of the N terminus of Kir2.2 were replaced by the corresponding domain of Kir2.1. By contrast, exchanging only the first 44 residues of the Kir2.2 N terminus did not diminish the effect of SGK3. These findings indicate that the C terminus and the residues 45–78 of the N terminus of Kir2.2 are required to confer SGK3 sensitivity.

In a second approach, we tried to introduce SGK3 sensitivity into the SGK3-insensitive Kir2.1 by transplantation of homologous regions of Kir2.2. SGK3-sensitive Kir2.1 channels could not be generated by single transplantations of the first 44 or 78 N-terminal residues or the whole C terminus from Kir2.2. However, simultaneous transplantation of both the N terminus (residues 1–78) and the C terminus from Kir2.2 to

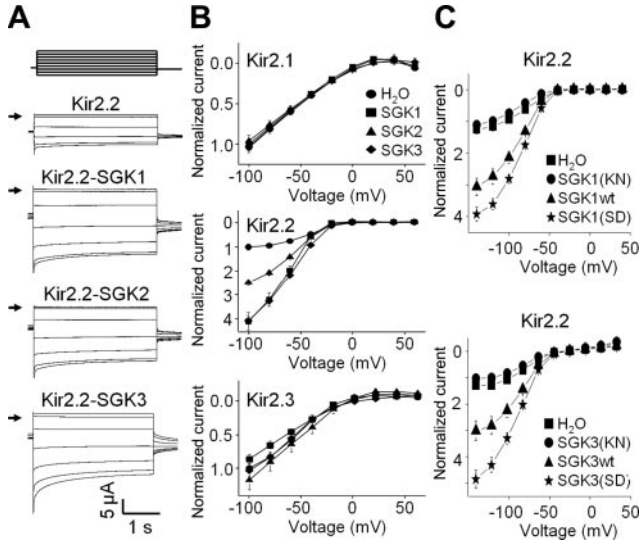

Figure 2. Active SGKs stimulate Kir2.2. Kir2 channels were expressed in *Xenopus* oocytes, and currents were recorded under voltage clamp in high-potassium solution (KD60) at potentials between −100 and +60 mV in 20-mV increments as depicted by the pulse protocol in panel *A*. Current amplitudes were determined at the end of 3 s pulses and normalized to the amplitude of the respective channel at −100 mV in the absence of SGK. *A*) Representative current traces of Kir2.2 in the absence or presence of SGK1, SGK2, or SGK3. Arrows indicate 0 current level. *B*) Current-voltage relationships of Kir2.1, Kir2.2, and Kir2.3 in the absence or presence of SGK1, SGK2, or SGK3. Data are shown as means ± SE; n = 6–35. *C*) Current-voltage relationships of Kir2.2 expressed alone or in combination with either wild-type, constitutively active (SD), or inactive (KN) SGK1 (top panel) or SGK3 (bottom panel). Data are shown as means ± SE; n = 5–30.

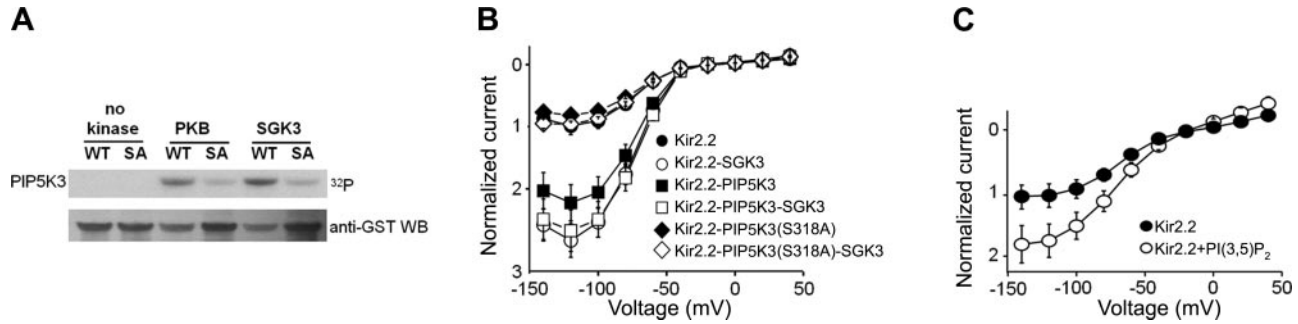

Figure 3. SGK3 phosphorylates recombinant PIP5K3 on Ser318 to stimulate Kir2.2 channels *via* $PI(3,5)P_2$. *A*) Recombinant GST-tagged wild-type PIP5K3 (WT) and mutant PIP5K3(S318A) (SA) were incubated with radioactive [γ-^{32}P]ATP in the absence or presence of PKB or SGK3 and analyzed by SDS-PAGE and Western blot. Top panel: representative autoradiogram of the blot membrane illustrating incorporation of radioactive phosphate. Bottom panel: same membrane probed with an anti-GST antibody. Images are representative of 2 independent experiments. *B*) Current-voltage relationships of Kir2.2 expressed in *Xenopus* oocytes alone or together with SGK3, PIP5K3, or inactive PIP5K3(S318A) in various combinations. Currents were recorded at potentials between −140 and +40 mV in 20-mV increments in KD60 recording solution. Current amplitudes were determined at the end of 3-s pulses. Data are shown as means ± SE; n = 24–35. *C*) Current-voltage relationships of Kir2.2 recorded and evaluated as in panel *B* in the absence of $PI(3,5)P_2$ and after injection of 2.3 ng $PI(3,5)P_2$; n = 21–25.

Kir2.1 resulted in SGK3-sensitive chimeric channels (Supplemental Fig. S2 and Fig. 4), supporting the conclusion that both the C terminus and the N terminus of Kir2.2 are involved in SGK3 sensitivity.

Stimulation of native SGK increases plasma membrane localization of EGFP-Kir2.2 in HEK and HeLa cells

Next, we explored whether the increase in Kir2.2 current produced by SGK was caused by a change in

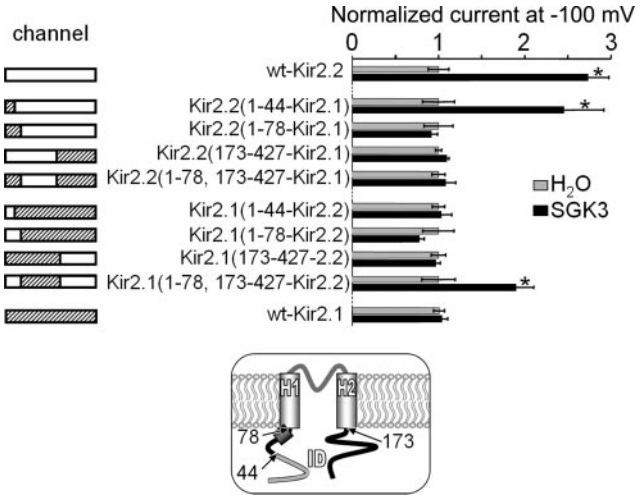

Figure 4. Stimulation by SGK3 depends on the N and C termini of Kir2.2. Kir2.1-Kir2.2 chimeric channels were expressed in *Xenopus* oocytes alone (solid bars) or in combination with SGK3 (shaded bars). Cartoons at left depict the respective chimeras. Currents were recorded at a potential of −100 mV in KD60 recording solution; amplitudes were determined at the end of 3-s pulses and normalized to the mean amplitude of currents in the absence of SGK3. Data are shown as means ± SE; n = 6–35. Inset: cartoon of a Kir2 subunit with regions conferring SGK3 sensitivity shown in black. Outer helix (H1), inner helix (H2), and intracellular domain (ID) are marked.

open probability or by modulation of surface expression of the channel. HeLa and HEK293 cells transfected with EGFP-tagged Kir2.2 were incubated in either serum-free medium or serum-containing medium supplemented with 3 μM dexamethasone to stimulate endogenous SGK. In both cell types, incubation with serum and dexamethasone gave rise to an increase in fluorescence at the plasma membrane (**Fig. 5**). In HeLa cells, increased plasma membrane localization of Kir2.2-EGFP was already observed 10 min after addition of serum and dexamethasone (Fig. 5*A*, *B* and Supplemental Fig. S1). These results demonstrate that at least part of the SGK-induced increase in Kir2.2-mediated currents is caused by an increase in cell surface expression (Fig. 5*C*).

Heteromeric Kir2.1, Kir2.2, and Kir2.3 channels are activated by SGK3

As mentioned above, Kir2.1 and Kir2.3 channels alone are insensitive to SGK1–3. However, all members of the Kir2 subfamily are coexpressed in cardiac ventricular muscle, skeletal muscle, brain, and other tissues (1) and form functional heteromers (3). Therefore, we studied the effects of SGK3 on heteromeric Kir2.x channels. When Kir2.2 was coexpressed with Kir2.1 or Kir2.3, or with both Kir2.1 and Kir2.3 to form heteromeric channels, part of the sensitivity of Kir2.2 to SGK3 was retained in the heteromeric channel complexes (**Fig. 6*A***). These results were confirmed by analyzing membrane localization of Kir2.1 using a luminometric assay (37): While SGK3 did not alter surface expression of HA-tagged Kir2.1 expressed alone in *Xenopus* oocytes, it boosted Kir2.1 surface expression when Kir2.2 was coexpressed, suggesting that SGK3 increases the trafficking of heteromeric complexes consisting of Kir2.1 and Kir2.2 channels to the plasma membrane (Fig. 6*B*).

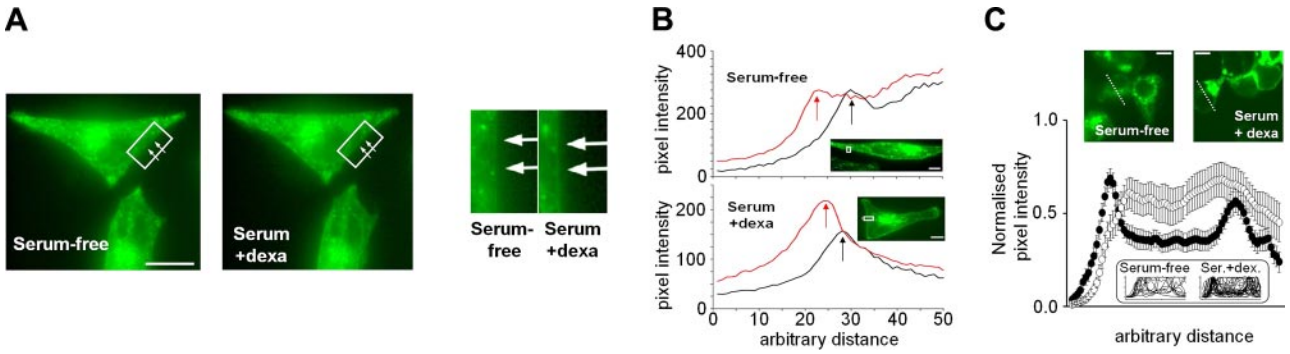

Figure 5. Stimulation of native SGK modulates EGFP-Kir2.2 localization in HeLa and HEK293 cells. *A*) Left panels: representative images of a HeLa cell expressing EGFP-tagged Kir2.2 taken before and after a 10-min exposure to 10% FCS plus 3 μM dexamethasone. Right panel: enlargements of boxed regions in left panels. Arrows indicate position of the cell membrane. *B*) Images of EGFP-Kir2.2-transfected HeLa cells show typical line profiles for the control that was incubated in FCS/dexamethasone-free medium (black lines). Top cell was incubated in FCS/dexamethasone-free medium, and the bottom cell was exposed to 10% FCS plus 3 μM dexamethasone-enriched medium. Red lines show the profiles 10 min after additions of the respective solution. Black line of bottom experiment refers to image that was taken at the beginning of the 10-min movie (Supplemental Video S1); red line shows the profile 10 min after addition of 10% FCS and 3 μM dexamethasone. Arrows indicate position of the cell membrane. *C*) Representative images of HEK293 cells expressing EGFP-tagged Kir2.2. To stimulate endogenous SGK, transfected cells were incubated for 40 min in medium containing 10% serum and 3 μM dexamethasone, while control cells were incubated in serum-free medium. Pixel intensities were determined for individual cells of similar sizes along a line across the cell, background intensity was subtracted, and data were normalized to the maximal intensity. Normalized intensity profiles (open circles for control cells; solid circles for cells stimulated with serum and dexamethasone) obtained from 42–53 cells were then averaged. Inset: overlaid intensity profiles of the individual cells. Ser.+dex., serum+dexamethasone. Data are presented as means ± SE. Scale bars = 5 μm.

SGK3 has diverse effects on Kir2 channels containing ATS-associated Kir2.1 mutants

To maximize effects and simplify interpretations for ATS, we individually coexpressed 10 different homomeric ATS-associated mutants of Kir2.1 with Kir2.2 and Kir2.3 in *Xenopus* oocytes. The resulting currents had small amplitudes because of the (variable) dominant-negative effects of Kir2.1 mutants (ref. 38 and Fig. 6*C*). Coexpression of SGK3 had diverse effects on the different heteromeric channels: it increased current amplitudes of four of the heteromers, whereas it did not significantly affect four others, and even inhibited two heteromers, namely those containing Kir2.1(V302M) and Kir2.1(E303K) (Fig. 6*C*).

Reducing the number of available inwardly rectifying K^+ channels leads to membrane depolarization and decrease of the extracellular K^+ concentration

We developed a computer model that allows simulation of transitions from normal to paralyzed states in skeletal muscle cells characteristic of patients with ATS. The model structure is described briefly in Supplemental Data. To assess the pathophysiological consequences of the effects of glucocorticoids on ATS-mutated Kir channels for the stability of the resting membrane potential and extracellular K^+ concentration, we simulated a reduction of the maximal inwardly rectifying K^+ conductance, reflecting a reduction either in the number of channels in the plasma membrane or in the open probability of channel activity in ATS channels (**Fig. 7*A***). According to our model, a fast transition of the plasma membrane from the normal to a depolarized state occurs when Kir channel conductance drops below 50%. This transition is paralleled by a shift of K^+ from the extracellular to the intracellular space.

DISCUSSION

SGK1–3 play a prominent role in cell growth and survival, regulation of energy metabolism, and many other cellular processes (39). Once activated by phosphorylation *via* the PI(3)P-dependent kinase PDK1, SGKs enhance the surface expression of several ion channels and transporters. However, the molecular mechanisms linking SGK activity and membrane trafficking are not yet fully understood.

Here we provide insight into the stimulation of inwardly rectifying potassium channels by SGKs. We show that the activation of SGK1 and SGK3, and to a lesser extent SGK2, substantially increases the inward currents mediated by homo- or heteromeric potassium channels containing the subunit Kir2.2 but not of those lacking Kir2.2. Increase in currents appears to be caused by an increase in the number of cell surface-expressed channels, as demonstrated by our experiments with GFP-tagged Kir2.2 in HeLa and HEK293 cells. Phosphorylation of PIP5K3 at serine 318 by SGK plays a crucial role in this signaling pathway. This is evidenced by our finding that neither the inactive mutant SGK3 nor wild-type SGK3 in combination with a phosphorylation-defective PIP5K3 mutant [PIP5K3(S318A)] is able to increase Kir2.2-mediated currents.

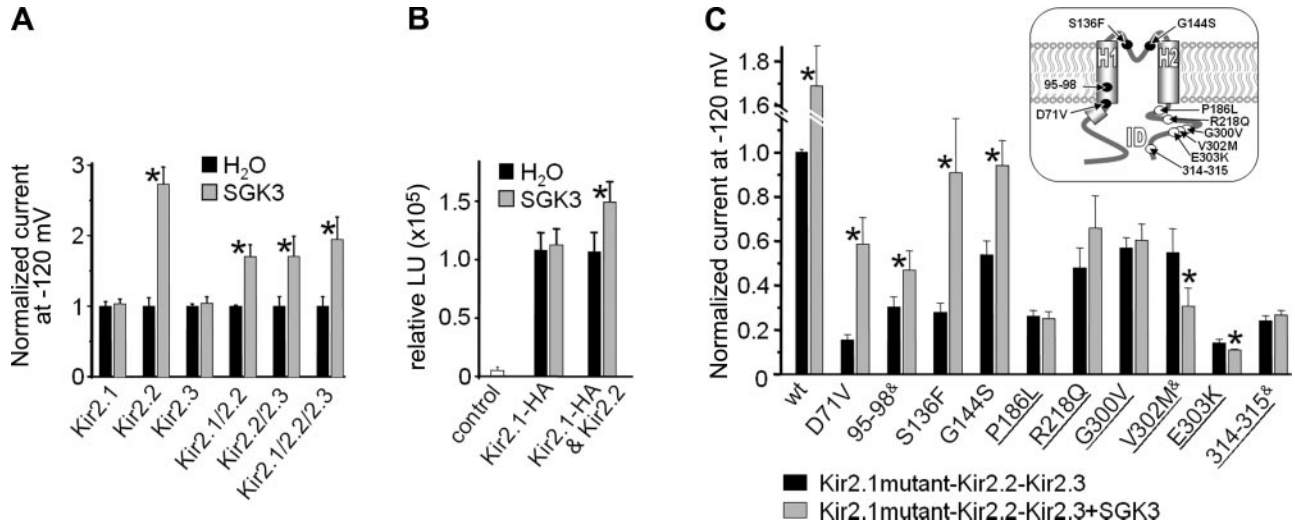

Figure 6. Kir2.2 confers SGK sensitivity to heteromeric Kir2 channel complexes. *A*) Kir2.1, Kir2.2, and Kir2.3 were coexpressed in various combinations with (shaded bars) or without SGK3 (solid bars). Current amplitudes were determined at the end of 3-s pulses to −120 mV in KD60 recording solution and normalized to the respective currents in the absence of SGK3; $n = 5–35$. *B*) HA-Kir2.1 was expressed alone or in combination with Kir2.2 and with or without SGK3, and surface membrane expression was assessed by a chemiluminescence assay; $n = 60$. *C*) Heteromeric Kir2.x channels containing the indicated Kir2.1 mutant subunits (aa 95–98, 314–315 are deletions) were coexpressed with (shaded bars) or without SGK3 (solid bars). Current amplitudes were determined at the end of 3-s pulses at −120 mV in KD60 recording solution and normalized to the mean amplitude of currents through Kir heteromers containing wild-type Kir2.1 subunits in the absence of SGK3; $n = 8–23$. Mutation in the Kir2.1 subunit is noted under the corresponding set of bars. Kir2.1 mutations that were reported to impair PIP_2 binding are underscored; those that impair channel trafficking are marked with ampersand (&). Inset: localization of mutations in the channel protein. Solid circles indicate positions of Kir2.1 mutations producing channels significantly stimulated on SGK3 coexpression; open circles indicate those producing channels with impaired SGK3 stimulation. Outer helix (H1), inner helix (H2), and intracellular domain (ID) are marked. Data are shown as means ± SE. $^*P < 0.05$.

PI(3)P, the substrate of PIP5K3, is a phospholipid residing primarily in membranes of early endosomes, where it can bind to a number of proteins, including PIP5K3 and SGK3, *via* their respective FYVE and PX domains. The coincident lipid binding of both proteins likely brings them into close proximity at the early endosomal membrane, thereby allowing phosphorylation and activation of PIP5K3 by SGK3. The activated PIP5K3, in turn, phosphorylates PI(3)P, yielding $PI(3,5)P_2$, which is typically localized in late endosomal compartments. Thus, we propose that the formation of $PI(3,5)P_2$ by SGK3-induced activation of PIP5K3 directs recycling endosomes to the cell surface, thereby facilitating trafficking of the channels back to the plasma membrane (Fig. 7*B*).

While the majority of recycled membrane proteins are directly shuttled back to the plasma membrane from early endosomes (40), some are first transported from the early endosomes to the (mostly perinuclear) endosomal recycling compartment (ERC) and later to the plasma membrane. The ERC is characterized by the presence of the small GTPase Rab11 (25, 40). Stimulation of PIP5K3 by SGK1 also enhances the surface expression of the voltage-activated K^+ channel KCNQ1/KCNE (41) *via* the Rab11-regulated pathway, suggesting that formation of $PI(3,5)P_2$ through PIP5K3 is of broader importance for recycling of membrane proteins to the plasma membrane (Fig. 7*B*). On the other hand, this pathway is also endowed with good degree of specificity, since the closely related Kir2.1 and Kir2.3 channels do not seem to pass the early endosome. Obviously, physical interaction of $PI(3,5)P_2$ with Kir2.2 (Fig. 2) mediates subtype specificity over Kir2.1 and Kir2.3.

Although it is not fully understood how SGK1 and SGK3 achieve selective enhancement of Kir2.2 trafficking, we found that the C terminus and the region between aa 45 and 78 of Kir2.2 are essential for its sensitivity to SGK3. It is likely that these regions are structurally affected by $PI(3,5)P_2$ binding. The transmembrane domains of Kir2.2 are apparently of reduced relevance for SGK3 sensitivity, since it can be transferred to Kir2.1 along with the N and C termini of Kir2.2. Alternatively, the transmembrane domains of Kir2.1 can substitute sufficiently for the transmembrane domains of Kir2.2 and therefore this region could not be detected by the chimeric approach used here.

As mentioned above, heteromeric Kir2 channels are only sensitive to SGK3 when they contain Kir2.2. Although the exact stoichiometry of the formed heteromers is not yet clear, the magnitude of the stimulatory effect suggests that one or two Kir2.2 subunits in the Kir2 tetramer are sufficient to provide sensitivity to SGK3 and PIP5K3. Mutant Kir2.1 subunits found in ATS exert dominant negative effects on the currents generated by the other Kir2 subunits (3, 42), which is also supported by our coexpression experiments of various ATS-associated Kir2.1 mutants with Kir2.2 and Kir2.3 channels. Surprisingly, the reduction in current

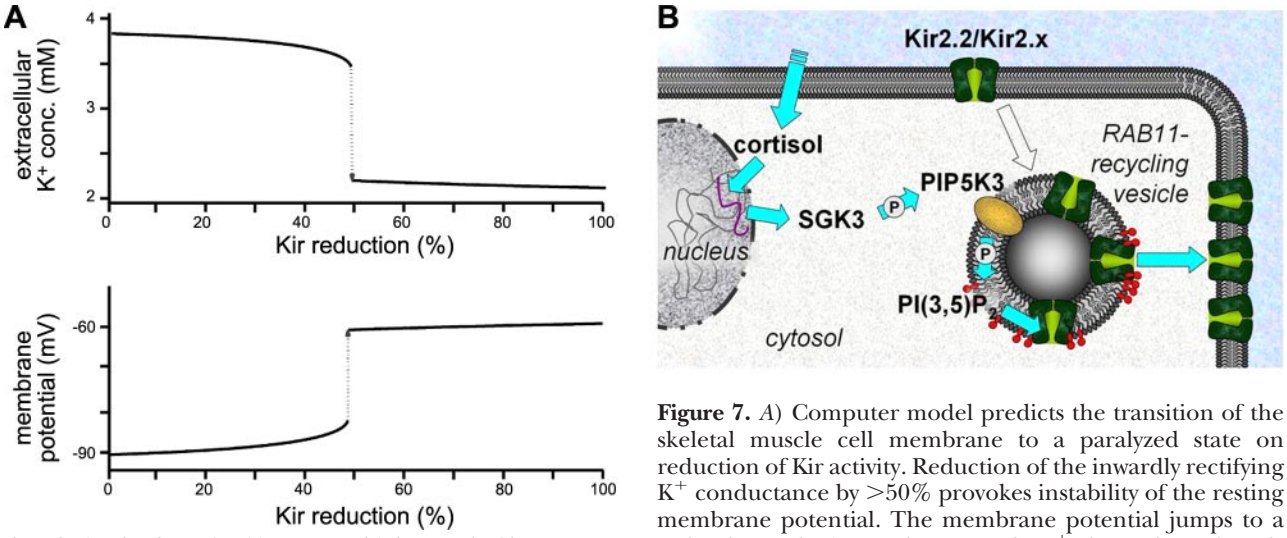

Figure 7. *A*) Computer model predicts the transition of the skeletal muscle cell membrane to a paralyzed state on reduction of Kir activity. Reduction of the inwardly rectifying K^+ conductance by >50% provokes instability of the resting membrane potential. The membrane potential jumps to a depolarized value of −60 mV, at which muscle fibers are expected to be weak, since voltage-gated Na^+ channels are largely inactivated. Concomitantly with transition of the membrane into the depolarized state, extracellular K^+ concentration drops rapidly, resulting in hypokalemia, which is characteristic for most patients during paralytic attacks. *B*) Model of Kir2 channel recycling. Schematic drawing shows that Kir2.2/Kir2.x channel exocytosis is enhanced by SGK3 and involves phosphorylation and activation of PIP5K3. Generated $PI(3,5)P_2$ may concentrate around Kir2.2/Kir2.x channels residing in RAB11-positive recycling vesicles and then trigger exocytosis. This process may be partly disrupted in Andersen-Tawil channels, possibly leading to accumulation in other intracellular compartments. Stimulation of SGK3/PIP5K3-dependent exocytosis leads to an increased membrane flux into the plasma membrane. This, in turn, will stimulate endocytosis to keep cell size constant. As some Andersen-Tawil channels are not enriched in RAB11-vesicles, their exocytosis is not stimulated, but instead they are endocytosed, resulting in reduced functional expression. If channel density drops below a critical value, the membrane shifts to a depolarized configuration, causing long-lasting inactivation of voltage-gated Na^+ channels and, as a consequence, paralysis of the muscle.

amplitude was partially reversed by coexpression with SGK3 in 40% of cases. There are two possible explanations for these observations: SGK3 increases the fraction of homomeric channels containing only Kir2.2 subunits, and/or SGK3 enhances surface expression of heteromeric channels containing both Kir2.2 and ATS-associated mutants of Kir2.1, as shown for Kir2.1/2.2 wild-type heteromeric channels (Fig. 6*B*).

Atrial myocytes, in contrast to ventricular myocytes, are characterized by a low density of background inwardly rectifying K^+ currents, which are related to both I_{K1} and agonist-independent GIRK currents. Low concentrations of Ba^{2+} can be used to identify the contribution of I_{K1} to the total background current, since at 2 μM I_{K1} is blocked by >70%, whereas GIRK currents are not affected (36). Treatment with serum plus dexamethasone resulted in an ~2-fold increase in the density of Ba^{2+}-sensitive I_{K1} (Fig. 1). On the contrary, the effect of SGK1 stimulation by serum plus dexamethasone in cultured human skeletal myotubes seems to be much smaller (~1.33-fold increase; $P=0.2$; $n=18/20$, data not shown).

The consequences of I_{K1} reduction on electrical activity of cardiac myocytes have been extensively studied by mathematical modeling (43). Reduction of I_{K1} was predicted to cause prolongations of the QT interval characteristic for the electrocardiogram of ATS patients, predisposing them to *torsade de pointes* arrhythmia and cardiac sudden death (43). Since comparable modeling studies in skeletal muscles were lacking so far, we generated a mathematical model that allowed us to predict the effects of changes in I_{K1} conductance on the electrical activity of skeletal muscle fibers. Our simulations of various degrees of I_{K1} reduction revealed that a reduction to less than ~50% goes along with a fast transition from the resting to a depolarized state (Fig. 7*C*). The transition was paralleled by a redistribution of K^+ and Cl^- ions from the extracellular to the intracellular space. A depolarization of the skeletal muscle membrane to potentials positive to −60 mV is known to cause muscle paralysis in hypokalemic and hyperkalemic periodic paralysis, since voltage-gated Na^+ channels are largely inactivated at these membrane potentials, rendering muscle fibers unexcitable and paralyzed.

ATS is characterized by a high degree of pleiotropy, and mutations in Kir2.1 can cause a reduction of inward rectifier currents by different molecular mechanisms (15, 38, 42, 44). The reported modulation of Kir2 channel function (and I_{K1}) by SGK isoforms may open novel therapeutic options for ATS. Depending on the underlying mutation, ATS patients may respond to alterations in SGK activity as induced by changes in blood glucose levels, psychological and mental stress, or systemic glucocorticoid treatment with either a partial rescue or even a further loss of function of I_{K1}. Pharmacological activation of SGK and PIP5K3 to increase I_{K1} might improve the symptoms in some patients with ATS. In a smaller subset of patients, inhibition of SGK and PIP5K3 may be indicated. Consistent with our results, corticosteroids have recently been suggested as po-

tent modifiers of periodic paralysis in patients with ATS (30). Based on our results, genotype-specific treatment targeting SGK and PIP5K3 might be required. FJ

This work was supported by the Deutsche Forschungsgemeinschaft (grants SE1077/3 to G.S., STR649/1-1 to N.S., La315/4-5 to F.L., DE1482/2-1 and DE1482/3-2 to N.D., and TP A4, SFB593 to J.D.), the P. E. Kempkes Foundation (grant 16/06 to R.P.M.), and the Association Française contre les Myopathies (grant to S.B.). F.L.H. is an endowed Senior Research Professor of the Gemeinnützige Hertie-Stiftung. The authors declare no conflicts of interest.

REFERENCES

1. Lopatin, A. N., and Nichols, C. G. (2001) Inward rectifiers in the heart: an update on I(K1). *J. Mol. Cell. Cardiol.* **33,** 625–638
2. Liu, Y., Liu, D., Heath, L., Meyers, D. M., Krafte, D. S., Wagoner, P. K., Silvia, C. P., Yu, W., and Curran, M. E. (2001) Direct activation of an inwardly rectifying potassium channel by arachidonic acid. *Mol. Pharmacol.* **59,** 1061–1068
3. Preisig-Müller, R., Schlichthorl, G., Goerge, T., Heinen, S., Brüggemann, A., Rajan, S., Derst, C., Veh, R. W., and Daut, J. (2002) Heteromerization of Kir2.x potassium channels contributes to the phenotype of Andersen's syndrome. *Proc. Natl. Acad. Sci. U. S. A.* **99,** 7774–7779
4. Beuckelmann, D. J., Näbauer, M., and Erdmann, E. (1993) Alterations of K^+ currents in isolated human ventricular myocytes from patients with terminal heart failure. *Circ. Res.* **73,** 379–385
5. Han, W., Chartier, D., Li, D., and Nattel, S. (2001) Ionic remodeling of cardiac Purkinje cells by congestive heart failure. *Circulation* **104,** 2095–2100
6. Kääb, S., Dixon, J., Duc, J., Ashen, D., Näbauer, M., Beuckelmann, D. J., Steinbeck, G., McKinnon, D., and Tomaselli, G. F. (1998) Molecular basis of transient outward potassium current downregulation in human heart failure: a decrease in Kv4.3 mRNA correlates with a reduction in current density. *Circulation* **98,** 1383–1393
7. Lodge, N. J., and Normandin, D. E. (1997) Alterations in I_{to}, I_{Kr} and I_{K1} density in the BIO TO-2 strain of syrian myopathic hamsters. *J. Mol. Cell. Cardiol.* **29,** 3211–3221
8. Collins, A., and Larson, M. (2002) Differential sensitivity of inward rectifier K^+ channels to metabolic inhibitors. *J. Biol. Chem.* **277,** 35815–35818
9. Collins, A., Wang, H., and Larson, M. K. (2005) Differential sensitivity of Kir2 inward-rectifier potassium channels to a mitochondrial uncoupler: identification of a regulatory site. *Mol. Pharmacol.* **67,** 1214–1220
10. Andersen, E. D., Krasilnikoff, P. A., and Overvad, H. (1971) Intermittent muscular weakness, extrasystoles, and multiple developmental anomalies. A new syndrome? *Acta Paediatr. Scand.* **60,** 559–564
11. Tawil, R., Ptacek, L. J., Pavlakis, S. G., DeVivo, D. C., Penn, A. S., Ozdemir, C., and Griggs, R. C. (1994) Andersen's syndrome: potassium-sensitive periodic paralysis, ventricular ectopy, and dysmorphic features. *Ann. Neurol.* **35,** 326–330
12. Plaster, N. M., Tawil, R., Tristani-Firouzi, M., Canun, S., Bendahhou, S., Tsunoda, A., Donaldson, M. R., Iannaccone, S. T., Brunt, E., Barohn, R., Clark, J., Deymeer, F., George, A. L., Jr., Fish, F. A., Hahn, A., Nitu, A., Ozdemir, C., Serdaroglu, P., Subramony, S. H., Wolfe, G., Fu, Y. H., and Ptacek, L. J. (2001) Mutations in Kir2.1 cause the developmental and episodic electrical phenotypes of Andersen's syndrome. *Cell* **105,** 511–519
13. Sansone, V., Griggs, R. C., Meola, G., Ptacek, L. J., Barohn, R., Iannaccone, S., Bryan, W., Baker, N., Janas, S. J., Scott, W., Ririe, D., and Tawil, R. (1997) Andersen's syndrome: a distinct periodic paralysis. *Ann. Neurol.* **42,** 305–312
14. Donaldson, M. R., Jensen, J. L., Tristani-Firouzi, M., Tawil, R., Bendahhou, S., Suarez, W. A., Cobo, A. M., Poza, J. J., Behr, E., Wagstaff, J., Szepetowski, P., Pereira, S., Mozaffar, T., Escolar, D. M., Fu, Y. H., and Ptacek, L. J. (2003) PIP_2 binding residues of Kir2.1 are common targets of mutations causing Andersen syndrome. *Neurology* **60,** 1811–1816
15. Rohacs, T., Chen, J., Prestwich, G. D., and Logothetis, D. E. (1999) Distinct specificities of inwardly rectifying K^+ channels for phosphoinositides. *J. Biol. Chem.* **274,** 36065–36072
16. Romanenko, V. G., Fang, Y., Byfield, F., Travis, A. J., Vandenberg, C. A., Rothblat, G. H., and Levitan, I. (2004) Cholesterol sensitivity and lipid raft targeting of Kir2.1 channels. *Biophys. J.* **87,** 3850–3861
17. Soom, M., Schonherr, R., Kubo, Y., Kirsch, C., Klinger, R., and Heinemann, S. H. (2001) Multiple PIP_2 binding sites in Kir2.1 inwardly rectifying potassium channels. *FEBS Lett.* **490,** 49–53
18. Xiao, J., Zhen, X. G., and Yang, J. (2003) Localization of PIP2 activation gate in inward rectifier K^+ channels. *Nat. Neurosci.* **6,** 811–818
19. Zitron, E., Kiesecker, C., Luck, S., Kathofer, S., Thomas, D., Kreye, V. A., Kiehn, J., Katus, H. A., Schoels, W., and Karle, C. A. (2004) Human cardiac inwardly rectifying current IKir2.2 is upregulated by activation of protein kinase A. *Cardiovasc. Res.* **63,** 520–527
20. Dart, C., and Leyland, M. L. (2001) Targeting of an A kinase-anchoring protein, AKAP79, to an inwardly rectifying potassium channel, Kir2.1. *J. Biol. Chem.* **276,** 20499–20505
21. Wischmeyer, E., Doring, F., and Karschin, A. (1998) Acute suppression of inwardly rectifying Kir2.1 channels by direct tyrosine kinase phosphorylation. *J. Biol. Chem.* **273,** 34063–34068
22. Berwick, D. C., Dell, G. C., Welsh, G. I., Heesom, K. J., Hers, I., Fletcher, L. M., Cooke, F. T., and Tavare, J. M. (2004) Protein kinase B phosphorylation of PIKfyve regulates the trafficking of GLUT4 vesicles. *J. Cell Sci.* **117,** 5985–5993
23. Jones, M. C., Caswell, P. T., and Norman, J. C. (2006) Endocytic recycling pathways: emerging regulators of cell migration. *Curr. Opin. Cell Biol.* **18,** 549–557
24. Jones, S. V. (2003) Role of the small GTPase Rho in modulation of the inwardly rectifying potassium channel Kir2.1. *Mol. Pharmacol.* **64,** 987–993
25. Leonoudakis, D., Conti, L. R., Radeke, C. M., McGuire, L. M., and Vandenberg, C. A. (2004) A multiprotein trafficking complex composed of SAP97, CASK, Veli, and Mint1 is associated with inward rectifier Kir2 potassium channels. *J. Biol. Chem.* **279,** 19051–19063
26. Leyland, M. L., and Dart, C. (2004) An alternatively spliced isoform of PSD-93/chapsyn 110 binds to the inwardly rectifying potassium channel, Kir2.1. *J. Biol. Chem.* **279,** 43427–43436
27. Nehring, R. B., Wischmeyer, E., Doring, F., Veh, R. W., Sheng, M., and Karschin, A. (2000) Neuronal inwardly rectifying K^+ channels differentially couple to PDZ proteins of the PSD-95/SAP90 family. *J. Neurosci.* **20,** 156–162
28. Sampson, L. J., Leyland, M. L., and Dart, C. (2003) Direct interaction between the actin-binding protein filamin-A and the inwardly rectifying potassium channel, Kir2.1. *J. Biol. Chem.* **278,** 41988–41997
29. Vicente, R., Coma, M., Busquets, S., Moore-Carrasco, R., Lopez-Soriano, F. J., Argiles, J. M., and Felipe, A. (2004) The systemic inflammatory response is involved in the regulation of K^+ channel expression in brain via TNF-alpha-dependent and -independent pathways. *FEBS Lett.* **572,** 189–194
30. Zerangue, N., Schwappach, B., Jan, Y. N., and Jan, L. Y. (1999) A new ER trafficking signal regulates the subunit stoichiometry of plasma membrane $K_{(ATP)}$ channels. *Neuron* **22,** 537–548
31. Seebohm, G., Strutz-Seebohm, N., Ureche, O.N., Henrion, U., Baltaev, R., Mack, A. F., Korniychuk, G., Steinke, K., Tapken, D., Pfeufer, A., Kääb, S., Bucci, C., Attali, B., Merot, J., Tavare, J. M., Hoppe, U. C., Sanguinetti, M. C., and Lang, F. (2008) Long QT syndrome-associated mutations in KCNQ1 and KCNE1 subunits disrupt normal endosomal recycling of I_{Ks} channels. *Circ. Res.* **103,** 1451–1457
32. Seebohm, G., Strutz-Seebohm, N., Baltaev, R., Korniychuk, G., Knirsch, M., Engel, J., and Lang, F. (2005) Regulation of KCNQ4 potassium channel prepulse dependence and current

amplitude by SGK1 in *Xenopus* oocytes. *Cell. Physiol. Biochem.* **16,** 255–262
33. Strutz-Seebohm, N., Seebohm, G., Shumilina, E., Mack, A. F., Wagner, H. J., Lampert, A., Grahammer, F., Henke, G., Just, L., Skutella, T., Hollmann, M., and Lang, F. (2005) Glucocorticoid adrenal steroids and glucocorticoid-inducible kinase isoforms in the regulation of GluR6 expression. *J. Physiol.* **565,** 391–401
34. Decher, N., Renigunta, V., Zuzarte, M., Soom, M., Heinemann, S. H., Timothy, K. W., Keating, M. T., Daut, J., Sanguinetti, M. C., and Splawski, I. (2007) Impaired interaction between the slide helix and the C-terminus of Kir2.1: a novel mechanism of Andersen syndrome. *Cardiovasc. Res.* **75,** 748–757
35. Bechem, M., Pott, L., and Rennebaum, H. (1983) Atrial muscle-cells from hearts of adult guinea-pigs in culture–a new preparation for cardiac cellular electrophysiology. *Eur. J. Cell. Biol.* **31,** 366–3695
36. Beckmann, C., Rinne, A., Littwitz, C., Mintert, E., Bösche, L. I., Kienitz, M. C., Pott, L., and Bender, K. (2008) G protein-activated (GIRK) current in rat ventricular myocytes is masked by constitutive inward rectifier current (I_{K1}). *Cell. Physiol. Biochem.* **21,** 259–268
37. Tristani-Firouzi, M., Jensen, J. L., Donaldson, M. R., Sansone, V., Meola, G., Hahn, A., Bendahhou, S., Kwiecinski, H., Fidzianska, A., Plaster, N., Fu, Y. H., Ptacek, L. J., and Tawil, R. (2002) Functional and clinical characterization of KCNJ2 mutations associated with LQT7 (Andersen syndrome). *J. Clin. Invest.* **110,** 381–388
38. Lang, F., Bohmer, C., Palmada, M., Seebohm, G., Strutz-Seebohm, N., and Vallon, V. (2006) (Patho)physiological significance of the serum- and glucocorticoid-inducible kinase isoforms. *Physiol. Rev.* **86,** 1151–1178
39. Arteaga, M. F., Wang, L., Ravid, T., Hochstrasser, M., and Canessa, C. M. (2006) An amphipathic helix targets serum and glucocorticoid-induced kinase 1 to the endoplasmic reticulum-associated ubiquitin-conjugation machinery. *Proc. Natl. Acad. Sci. U. S. A.* **103,** 11178–11183
40. Seemann, G., Sachse, F. B., Weiss, D. L., Ptacek, L. J., and Tristani-Firouzi, M. (2007) Modeling of I_{K1} mutations in human left ventricular myocytes and tissue. *Am. J. Physiol. Heart Circ. Physiol.* **292,** H549–H559
41. Dunker, N., Schmitt, K., and Krieglstein, K. (2002) TGF-beta is required for programmed cell death in interdigital webs of the developing mouse limb. *Mech. Dev.* **113,** 111–120
42. Bendahhou, S., Fournier, E., Gallet, S., Menard, D., Larroque, M. M., and Barhanin, J. (2007) Corticosteroid-exacerbated symptoms in an Andersen's syndrome kindred. *Hum. Mol. Genet.* **16,** 900–906
43. Seemann, G., Sachse, F. B., Weiss, D. L., Ptácek, L. J., and Tristani-Firouzi, M. (2007) Modeling of I_{K1} mutations in human left ventricular myocytes and tissue. *Am. J. Physiol. Heart Circ. Physiol.* **292,** H549–559
44. Sarkar, G., and Sommer, S. S. (1990) The "megaprimer" method of site-directed mutagenesis. *Biotechniques* **8,** 404–407

Received for publication August 18, 2011.
Accepted for publication September 30, 2011.